HHS Public Access

Author manuscript

AJR Am J Roentgenol. Author manuscript; available in PMC 2020 August 18.

Published in final edited form as:

AJR Am J Roentgenol. 2015 September ; 205(3): 502–512. doi:10.2214/AJR.15.14463.

Regional Articular Cartilage Abnormalities of the Hip

Thomas M. Link[1], **Benedikt J. Schwaiger**[1], **Alan L. Zhang**[2]

[1]Department of Radiology and Biomedical Imaging, University of California at San Francisco, 400 Parnassus Ave, A-367, San Francisco, CA 94131

[2]Department of Orthopedic Surgery, University of California at San Francisco, San Francisco, CA

Abstract

OBJECTIVE.—Imaging of hip cartilage is challenging because of its limited thickness and complex geometry and therefore requires advanced MRI techniques. However, cartilage abnormalities are found in a number of disease entities, and their diagnosis may impact patient management. This article will provide pertinent information about the motivation to image hip cartilage, which imaging techniques to use, and how to analyze cartilage; finally, we will discuss disease entities with regional cartilage lesions, including the typical MRI findings.

CONCLUSION.—Because the detection and quantification of regional cartilage abnormalities are critical for guidance of operative and nonoperative management of hip disorders, radiologists should be familiar with imaging and analysis techniques for assessing hip cartilage.

Keywords

cartilage; femoroacetabular impingement; hip; MRI; quantitative imaging; T1rho; T2 relaxation time

Regional articular cartilage abnormalities are associated with hip pain and disability [1], and they are also seen in disorders such as femoroacetabular impingement (FAI), trauma, and insufficiency fractures, all of which can result in osteoarthritis and eventually total hip replacement [2].

Purpose and Scope

This article aims to provide background information about why the diagnosis of focal abnormalities of the hip cartilage may play a critical role in preventing total joint replacement, to inform the reader about morphologic and compositional MRI techniques, to explain how to characterize cartilage abnormalities, and to outline typical disease entities associated with regional cartilage abnormalities.

Address correspondence to T. M. Link (tmlink@radiology.ucsf.edu).

Background: Why Is It So Important to Diagnose Regional Cartilage Abnormalities?

Over the past 20 years substantial progress has been made in understanding the causes of hip joint disorders and developing new treatment options. New biomechanical concepts have evolved suggesting that a high percentage of cases of hip osteoarthritis, which was initially thought to be an idiopathic disorder, are in fact related to instability and impingement [3]. In particular, recognizing the significance of FAI has impacted our understanding of the pathophysiology of early hip osteoarthritis [4], although there are still significant controversies in this field [5]. Twenty years ago, therapy for articular cartilage lesions was limited, and progression of the disease would have eventually resulted in total hip arthroplasty (THA). Currently, the new operative and arthroscopic techniques that have evolved aim to prevent and slow the progression of hip osteoarthritis [6].

The detection of early abnormalities of the hip cartilage, which can be treated, requires sensitive imaging techniques. MRI has increasingly been used for this purpose because it shows internal joint derangement directly. Detection and quantification of regional cartilage abnormalities, labral tears, and bony anatomic abnormalities are critical to guide operative and nonoperative management of hip disorders [7]. Diagnosing and quantifying the extent of focal cartilage lesions at the hip will impact patient management, particularly in patients with FAI, chondral injuries, and insufficiency fractures, and will aid in the prevention of cartilage degeneration and disease progression.

Femoroacetabular Impingement

The presence and extent of cartilage lesions guide arthroscopic surgery in patients with FAI. Because FAI lesions are common in young athletes, it is important to assess cartilage injuries in these patients. Operative therapy options hold more promise of success in earlier stages of this disease, so any signs of cartilage injury could lead to a greater urgency in surgical invention for FAI lesions.

Chondral Injuries

Chondral injuries treated with cartilage repair techniques of the hip such as microfracture, autologous chondrocyte implantation, and mosaicplasty require exact preoperative visualization to optimally plan the repair procedures [8]. Furthermore, it is important to counsel patients in the preoperative setting about the possible need for cartilage repair because these procedures require prolonged rehabilitation protocols after surgery. Preoperative counselling is also needed in patients undergoing surgery for other diseases, such as FAI, in which concomitant full-thickness cartilage injury or delamination are detected and may necessitate extended surgical treatment.

Insufficiency Fractures

In insufficiency fractures, the size of the focal cartilage lesions directly impacts the prognosis of patients; it has been shown that large cartilage lesions overlying the insufficiency fracture will more likely require total joint replacement [9]. If the cartilage is normal or if only small cartilage lesions are identified, conservative management will be

more successful and should be the first-line treatment; hence, cartilage assessment will impact patient management.

Prevention

Epidemiologic studies have shown that focal cartilage lesions progress over time and that obesity and high-impact physical activities are associated with cartilage degeneration [10, 11]. Lifestyle changes have a significant influence on disease progression [12], and early detection of cartilage damage and patient education therefore may delay hip replacement. This emphasis on patient education is noteworthy because currently no pharmacotherapies are available to effectively treat cartilage damage.

Imaging Techniques: Which Techniques Are Required to Image Regional Cartilage Abnormalities of the Hip?

Imaging of the hip joint cartilage is challenging because the cartilage is thin, ranging from 1.3 mm (superomedial) to 3.0 mm (superolateral) at the acetabulum and from 2.3 mm (superomedial) to 0.8 mm (superolateral) at the femoral head in healthy individuals [13]. Also, separation of the two cartilage layers is challenging, and high-resolution imaging with good signal-to-noise ratios (SNRs) is required to visualize the hyaline cartilage best.

To date, there are no dedicated hip surface coils for MRI, and the best coils for imaging of a single hip are cardiac or “flex” coils, which are available from different manufacturers. The coils that usually provide better image quality are phased-array coils with multiple channels (8–32). Multichannel phased-array torso coils may be used for imaging of bilateral hips, but this technique is of limited use for the assessment of hip cartilage because the spatial resolution and SNR are inferior to the examination with a smaller-FOV coil. Given that the hip joint is relatively deep within the pelvis, image quality can also be enhanced by increasing the field strength; imaging at 3 T is currently best suited to visualize hip hyaline cartilage [14, 15].

Sequences

MRI protocols should allow a reproducible and valid assessment of cartilage while providing maximum information about the other joint structures [16]. Focal cartilage lesions are adequately detected on fast spin-echo (FSE) sequences, which are either intermediate-weighted (TE range = 30–60 ms) or proton density–weighted (TE range = 10–30 ms) [17–19]. A number of studies and protocol recommendations comprise fat-suppressed (FS) sequences in at least two planes [18, 20–23], whereas others have used no fat suppression [24, 25], especially when metallic orthopedic hardware was present [26].

A recent study showed good results for cartilage evaluation with a 3D proton density-weighted FS FSE sequence with variable flip angle after autologous chondrocyte transplantation [27]. Also, an intermediate-weighted 3D FSE sequence with isotropic resolution (Cube, GE Healthcare) was shown to detect cartilage lesions with a significantly higher sensitivity than a routine protocol [28], and this technique was optimized regarding image quality and motion artifacts [29]. Three-dimensional FSE sequences with isotropic

spatial resolution allow reconstructions in arbitrary imaging planes and are currently adapted to hip cartilage imaging; the preliminary results with these sequences are promising, as shown in Figure 1. Cartilage delineation—especially separation of femoral and acetabular cartilage—may be improved by using these sequences.

Three-dimensional gradient-echo sequences are also used for cartilage imaging, including FS 3D FLASH [30], 3D spoiled gradient-recalled echo [31], and 3D dual-echo in the steady state (DESS) [32] sequences. Spoiled T2*-weighted multiecho gradient-echo sequences including MERGE (Multiple Echo Recombined Gradient Echo, GE Healthcare), MEDIC (Multi-Echo Data Image Combination, Siemens Healthcare), and M-FFE (Merged Fast Field Echo, Philips Healthcare) are available. These sequences are useful for both volumetry and T2* relaxation time analyses of cartilage [33, 34]. In the knee, these sequences provide good delineation of articular cartilage and therefore are suitable for quantitative assessment of cartilage volume and thickness [23]. However, given the technical and anatomic challenges of hip MRI, the delineation of cartilage from synovial fluid in the hip is inferior with 3D gradient-echo sequences compared with intermediate-weighted 2D sequences. Also, to achieve an SNR with sufficient cartilage signal intensity, long scanning times are necessary [35] and artifacts are more prominent in the 3D sequences mentioned [36]. Therefore, in clinical routine, 3D gradient-echo sequences are limited in assessing cartilage structure and surface abnormalities as shown in Figure 2.

Coronal sequences allow optimal evaluation of the suprafoveal femoral head and lateral acetabular dome, whereas the cartilage over the anterior and posterior walls can be visualized best on axial images. Sagittal images are primarily used for the detection of labral abnormalities; they are also particularly suitable for the evaluation of the weight-bearing portion of the cartilage of the femoral head and acetabular dome [2]. These regions are prone to cartilage lesions, especially in patients with FAI, avascular necrosis, and insufficiency fractures, and therefore should be assessed with special attention [15, 37, 38].

MR Arthrography

In 2004, a study reported the detection of cartilage lesions of the hip on 2D proton density-weighted FS FSE sequences with a sensitivity of only 18%, whereas the sensitivity of direct MR arthrography was significantly higher at 41% [39]. Although that study advocated MR arthrography as being the superior diagnostic technique, the patient numbers were relatively low and scanning was performed at 1.5 T. A more recent study by Sutter et al. [40] compared MRI and MR arthrography in detecting cartilage lesions separately of the acetabulum and femoral head. Using standard MRI with FS intermediate-weighted FSE and DESS sequences, they reported sensitivity for acetabular cartilage lesions of 58% (reader 1) and 83% (reader 2) (specificity, 100% and 50%, respectively) and sensitivity for femoral cartilage defects of 50% (reader 1) and 83% (reader 2) (specificity, 100% and 59%). The sensitivities of MR arthrography were higher for acetabular lesions with sensitivity of 71% (reader 1) and 92% (reader 2) (specificity, 100% and 25%) but were similar for femoral cartilage defects, with sensitivity of 50% (reader 1) and 83% (reader 2) (specificity, 91% and 46%). This recent study impressively shows the challenges in analyzing cartilage lesions at the hip joint. In another recent study, the sensitivity of MR arthrography was reported to be

65% [41], which is in agreement with a pooled sensitivity of 62% and specificity of 86% reported in the review by Smith et al. [42]. High accuracies for the detection of chondral and labral lesions under weight-adapted traction of the hip joint were recently reported, suggesting that the diagnostic value of MR arthrography may further be improved [43].

Protocol Recommendations

Protocol recommendations for routine clinical imaging of articular cartilage of the hip for 1.5- and 3-T MRI are shown in Table 1. In general, we recommend intermediate-weighted sequences with fat suppression, a high matrix size, and thin sections (3—4 mm). Individual parameters have to be chosen differently for 1.5 and 3 T to reflect inherent differences in SNR. We acquire these sequences in coronal, sagittal, and oblique axial imaging planes. If MR arthrography is performed, coronal Tl-weighted imaging sequences are added to the sequences as shown in Table 1.

Compositional Imaging

None of the conventional morphologic MRI sequences described is capable of detecting molecular and biochemical changes in cartilage [44]. In particular, a decreased glycosaminoglycan content and an increased water content in the extracellular matrix precede morphologic cartilage lesions [45] and may be diagnosed at a potentially reversible stage [46, 47].

Delayed gadolinium-enhanced MRI of cartilage (dGEMRIC) uses a T1 mapping technique after the IV administration of gadopentetate dimeglumine [48]. Because of their negative charge, glycosaminoglycans repulse the negatively charged contrast agent; thus, in areas with depleted glycosaminoglycan concentration, an accumulation of contrast material can be detected [49]. Already established in knee research [50, 51], these observations were reproduced in the hip [52]. However, an IV injection of gadopentetate dimeglumine is required followed by temporary exercise to distribute the gadolinium.

The spin lattice relaxation time in the rotating-frame technique, which is known as “T1rho,” is an alternative noninvasive imaging technique. Being sensitive to regional changes in proteoglycans [53], T1rho imaging has been used mostly to assess knee cartilage, especially in early stages of osteoarthritis [18, 54], but its feasibility and clinical relevance in the hip have been reported [55–57]. The T1rho color maps of a healthy volunteer and a patient with early hip osteoarthritis shown in Figure 3 reveal the differences in biochemical composition.

T2 relaxation times relate to the rate of transverse magnetization and to the rate of the nuclear MR decay of nuclei, which are caused by the loss of phase coherence induced by a preceding radiofrequency pulse [58]. The water content and collagen content of the extracellular matrix and its orientation influence T2 relaxation times. This effect has been used to assess cartilage composition in healthy volunteers and in patients with hip dysplasia, FAI, and hip osteoarthritis [57, 59, 60]. T2* mapping is a technique similar to T2 mapping, but T2* mapping has shorter scanning times and is more sensitive to susceptibility artifacts [61]. In the hip, Bittersohl et al. [34, 61] found a significant correlation between T2* relaxation times and dGEMRIC and histologic assessments of the cartilage, respectively.

Other studies have shown that the T2* values of healthy volunteers significantly differed from those of patients with FAI [62, 63].

A recent study found that analysis of T2 and T1rho values separately assessed in local regions were more sensitive than global measurements of the cartilage composition of the hip and were consistent with region-specific cartilage degeneration [57]. This finding emphasizes the fact that compositional imaging parameters should be assessed in a region-specific approach to better characterize regional variations in cartilage composition and degeneration. However, to date, compositional imaging is used predominantly in a research setting. However, given the potential of these techniques to detect hip cartilage abnormalities in a possibly reversible stage, they may be performed in clinical practice in the near future.

Hip Cartilage Analysis: How Can Regional Hip Cartilage Abnormalities Be Assessed?

There are several types of focal abnormalities including focal cartilage defects, focal swelling of cartilage, osteochondral lesions, and delamination. Delamination is a typical sign in FAI, and the imaging findings will be discussed in detail. Focal swelling of cartilage is shown by increased signal intensity but may be difficult to visualize because of the limited thickness of the hip cartilage. Cartilage defects and injuries may be partial or complete with or without an abnormality of the underlying subchondral bone. To quantify the severity of cartilage lesions, the Outerbridge and Noyes classifications, based on surgical and arthroscopic evaluations, respectively [64, 65], have been modified to grade MRI findings in knee and hip cartilage [41, 62, 66, 67]. These MRI scores assess the depth of the cartilage damage and distinguish among superficial partial-thickness lesions (< 50%); deep partial-thickness lesions (> 50%); and full-thickness lesions, which are consistent with complete cartilage denudation. At the hip, differentiation of deep from superficial cartilage lesions is challenging [68]. These Outerbridge and Noyes classifications do not include the size of the lesions; however, after trauma and if cartilage repair is considered, exact measurement of lesion size is required and needs to be provided to the orthopedic surgeon to plan surgical intervention. Osteochondral lesions have a cartilage defect associated with an underlying bony abnormality, such as a bone marrow edema pattern, subchondral cyst, or bony defect. Typically, osteochondral lesions are posttraumatic but may also be degenerative.

More recently, several whole-joint MRI scoring systems have been developed to more comprehensively score cartilage and associated joint abnormalities; the key features of these systems are shown in Table 2. The earliest comprehensive whole-organ hip osteoarthritis scoring system was developed by Neumann et al. [69]; their system focused on assessing cartilage, bone marrow signal changes, labral tears, osteophytes, and subchondral cysts using direct MR arthrography [69]. However, this scoring system requires direct MR arthrography and to date has not been sufficiently validated [69, 70].

The Hip Osteoarthritis MRI Scoring System (HOAMS) [70] assesses similar features as the grading system by Neumann et al. [69] but also analyzes synovitis and joint effusion. Cartilage of both layers—the femur and acetabulum—are assessed together in one score after subdividing four zones in the sagittal plane and five zones in the coronal plane. Interreader agreement was good, and some features of HOAMS correlated significantly with Kellgren-Lawrence grades on hip radiographs [70].

Most recently, the evaluation system known as “SHOMRI” (scoring hip osteoarthritis with MRI) based on unenhanced 3-T MRI was presented by Lee et al. [21]. This whole-organ score analyzes eight features including articular cartilage loss, bone marrow edema pattern, subchondral cysts, and labral abnormalities. Articular cartilage loss, bone marrow edema pattern, and subchondral cysts are graded in 10 subregions on the basis of the geographic zone method established by the International Society for Hip Arthroscopy [71]. In each subregion, cartilage lesions are scored using a 3-point scale ranging from no cartilage loss, partial-thickness loss, to full-thickness loss. SHOMRI showed good to excellent reproducibility and significant correlations with both radiography-based osteoarthritis grading systems and clinical parameters. However, this scoring system has not been validated using arthroscopy or pathology. Figure 4 shows how scoring is performed using SHOMRI on a coronal fluid-sensitive FSE image. Although these semiquantitative scoring systems are currently not routine clinical practice, they will be used for clinical trials and radiologists need to be familiar with them.

Regional Abnormalities of the Hip: What Are the Disease Entities Associated With Regional Cartilage Damage?

Femoroacetabular Impingement

One of the entities with regional cartilage abnormalities that has been identified as a major contributor in the cause of early osteoarthritis is FAI [4, 72]. Cam-type FAI and pincer-type FAI have been differentiated: Each type presents cartilage injury in different regions.

Cam-type impingement——Cam-type impingement is characterized by abnormal head-neck morphology in which there is an osseous prominence at the head-neck junction that can lead to anterosuperior labral tears and anterosuperior cartilage injury [73]. The osseous prominence can be quantified using the alpha angle on oblique axial MR images; however, there is substantial overlap in the alpha angle measurements of healthy volunteers and patients with cam-type deformities [74, 75]. The anterosuperior segment has been recommended for this measurement because it discriminates between healthy subjects and subjects with FAI best [74, 75]. Sutter et al. [74] found that increasing the alpha angle threshold value from 55° to 60° significantly reduced falsepositive results, while maintaining a reasonable sensitivity. In a study by Kassarjian et al. [73], anterosuperior cartilage lesions were found in 95% (40/42) of the patients. Patients with symptomatic FAI typically have rapid cartilage loss over the anterosuperior margin of the dome and active delamination may be seen, which is manifested as hyperintensity in the basilar component of the cartilage over the anterior dome extending down to the tidemark [2, 24]. Figures 5–7 show examples of arthroscopically proven carpet lesion or delaminating lesion in patients with FAI. All three cases show a linear area of bright signal intensity along the acetabular subchondral bone covered by an area of darker tissue. These findings are typical but are relatively subtle, and they are seen on both MR arthrograms and standard MRI studies. Note that no contrast material is seen underneath the cartilage in the MR arthrograms (Fig. 5B and 6A), meaning that MR arthrography does not need to show injected contrast material within the cartilage substance to be reliable. Pfirrmann et al. [76] reported high specificity for the presence of hypointense areas in the acetabular substance on intermediate-weighted FS sequences in

patients with delamination confirmed at arthroscopy, which can also be seen in Figures 6 and 7. A typical arthroscopic finding in early FAI is the so-called “wave sign,” due to loss of fixation of the cartilage to the subchondral bone [77], which corresponds to the previously described delamination (Fig. 7). The overall diagnosis of delamination is difficult even with MR arthrography, and previous studies have reported sensitivities ranging between 22% and 74% [76, 78].

Pincer-type impingement——Pincer-type impingement is related to overcoverage of the femoral head and is typically associated with coxa profunda and acetabular retroversion [2]. Retroversion of the upper part of the acetabulum leads to the anterosuperior rim and lateralized medial edge abutting against the head-neck junction during flexion of the hip, whereas acetabular protrusion leads to anterior overcoverage of the head by the acetabulum [79]. Pfirrmann et al. [80] found that cartilage lesions in patients with pincer-type FAI were significantly larger at the posteroinferior position than cartilage lesions in patients with cam-type FAI. Pincer-type impingement typically manifests with primary labral failure followed by slower progressive cartilage loss [2]. Pincer-type FAI is more frequently found in women than in men and in older patients.

Traumatic Cartilage Injuries

Cartilage lesions are frequently related to sports injuries, as shown in a recent study in younger retired National Football League players [81]. In that study, chondral lesions were found in 98% (54/55) of the players [81]. Cartilage lesions were more frequent than labral tears or any other abnormality. Using arthroscopy in 29 patients as a standard of reference, Khanna et al. [82] showed that acute traumatic injury to the hip resulted in loose bodies (59%), intraarticular step deformities (38%), osteochondral lesions (49%), and labral tears (93%). Traumatic hip dislocation was shown to be frequently (20/32, 63%) associated with osteochondral impaction fractures [83], which typically result in posttraumatic osteoarthritis.

Different types of regional cartilage injuries have been described on MRI [84]: first, a focal cartilage signal abnormality, most consistent with edematous changes related to a contusion; second, a cartilage flap or flake fracture with a focal defect (Fig. 8) and a cartilage fragment that is attached to the remaining cartilage or separated (loose body); third, a focal subchondral fracture associated with cartilage damage; and, finally, osteochondral fractures, which are the most severe injuries and include a fragment containing both cartilage and bone. The latter may be associated with hip dislocation. Typically, acute cartilage injury is associated with the bone marrow edema pattern, labral tears, and joint effusion. The diagnostic performance of MRI for cartilage injuries is not as high in the hip as it is in the knee; in a recent study using arthroscopy as a standard of reference, 29% (4/14) of posttraumatic osteochondral lesions were missed on MRI [82].

Degenerative Changes

Although the definition of hip osteoarthritis is typically based on radiographs, focal cartilage loss is one of the key features of degenerative joint disease [85]. Teichtahl et al. [86] recently reviewed cartilage structural changes in adults (age range, 50–85 years) with and without hip osteoarthritis in a community-based setting. The diagnosis of hip osteoarthritis was based on

radiographic evidence (Kellgren-Lawrence grade ≥ 2) and clinical symptoms. Although subjects with osteoarthritis showed significantly more cartilage lesions, a high number of cartilage lesions were also found in asymptomatic subjects. At the femoral head, most lesions were found in the central superolateral region (17/19, 89.5%) in osteoarthritis subjects, whereas asymptomatic individuals typically had lesions in the central inferomedial region (67/141,47.5%) followed by the superolateral region (45/141, 31.9%). Subjects with osteoarthritis had lesions in more than 50% at all sites of the femoral head, whereas healthy individuals rarely had lesions in the anterior and posterior regions. Acetabular lesions were found in nearly all osteoarthritis patients—in particular, in the central superolateral and anterior regions (89.5%' and 94.7%, respectively); however, on average, lesions of the acetabular cartilage were found in only 25–30%' of the healthy subjects. Bone marrow abnormalities were found frequently in osteoarthritis subjects but rarely in healthy individuals. This study is of substantial importance because it shows a high prevalence of cartilage lesions in asymptomatic elderly subjects without signs of osteoarthritis; cartilage lesions, however, may be more typical for patients with osteoarthritis if the lesions are located in the acetabulum or if they are associated with bone marrow abnormalities. Figure 9 shows the typical location of cartilage defects in the central, superolateral, and anterior regions of the acetabulum in a patient with moderate hip osteoarthritis.

MRI also has an important indication in subjects with a radiographic diagnosis of hip osteoarthritis: It provides additional information that may impact the decision about whether to perform TH A. Currently most patients undergoing THA have only moderate osteoarthritis based on radiographs [87]. Additional more detailed information about the full extent of degenerative disease affecting the articular cartilage, bone marrow, labrum, and synovium may better help select patients for THA. Clearly, larger clinical trials providing evidence about how MRI could impact indications for THA are required.

Although a relatively high percentage of individuals with cartilage defects are asymptomatic [86], these degenerative changes may become symptomatic later in life. Given that macroscopic cartilage defects are considered irreversible, changes in the cartilage matrix ideally should be diagnosed even before focal cartilage lesions occur on a macroscopic scale. This additional information may be provided by compositional imaging using MRI techniques at earlier stages of degeneration when the changes would still be reversible [56, 76].

Subburaj et al. [57] showed significant differences in cartilage T1rho and T2 relaxation times in younger subjects with FAI and in those without FAI, particularly in the anterosupeiior region; these results document the potential role of compositional techniques in the diagnosis of degenerative disease in the early stages [57]. Because these techniques provide information about the biochemical composition of cartilage, they may be used as biomarkers to evaluate cartilage quality and the risk of developing osteoarthritis, similar to bone mineral density measurements that are used to predict osteoporotic fractures.

Compositional techniques could also allow physicians to monitor the effects of therapeutic interventions. Currently, these interventions include lifestyle modifications to prevent osteoarthritis and arthroscopic surgery for FAI. Intraarticular and oral pharmacotherapies

that may eventually provide effective treatment and halt the progression of osteoarthritis are under development.

Insufficiency Fractures

Subchondral insufficiency fractures of the hip have been identified as a cause of accelerated osteoarthritis [88]. Subchondral insufficiency fractures are typically found in older female patients with increased bone fragility. They may be associated with steroid use, radiation therapy, renal transplantation, and inflammatory arthropathies. This entity is distinct from avascular necrosis and characterized by subchondral collapse of the superolateral segment of the femoral head.

Characteristic MRI findings of subchondral insufficiency fractures include a low-signal-intensity band on T1- and T2-weighted images in the subchondral bone adjacent or parallel to the articular surface that is associated with an extensive surrounding bone marrow edema pattern [89]. High signal intensity proximal to the low-intensity band on fluid-sensitive sequences may help differentiate this entity from avascular necrosis [37], but sometimes a focal fracture deformity of the femoral head and a low-intensity band fused with the subchondral bone are detected simultaneously, as shown in Figure 10. Subchondral insufficiency fractures are frequently associated with focal cartilage defects, particularly if subchondral collapse is present, which leads to progressive osteoarthritis and frequently to total joint arthroplasty. The size of the cartilage defect is directly related to the prognosis and outcome of the patients: Large defects (mean ± SD, 29 ± 11.8 mm) are seen in patients with disease that progresses to THA, whereas patients with small defects (14 ± 8.5 mm) have a better prognosis and require THA less frequently [9].

Summary and Conclusion

Because detection and quantification of regional cartilage abnormalities are critical for the guidance of operative and nonoperative management of hip disorders, radiologists should be familiar with imaging and analysis techniques for assessing hip cartilage. In this article, we presented state-of-the-art and evolving imaging techniques for the evaluation of hip cartilage and discussed currently available semiquantitative and compositional analysis methods. We also focused on typical disease entities that are associated with cartilage damage and highlighted the typical imaging features of these lesions.

Acknowledgments

We thank Misung Han and Roland Krug (Musculoskeletal Quantitative Imaging Research [MQIR], Department of Radiology & Biomedical Imaging, University of California at San Francisco [UCSF]) for their support and for providing the 3D Cube images. We also thank Michael Samaan and Richard B. Souza (MQIR, UCSF) for providing the T1rho color maps. Thank you also to Alexandra S. Gersing for thoroughly proofreading the manuscript. We also thank Patrick D. Koon (GE Healthcare) for critically discussing MR sequences for imaging hip cartilage and providing his expertise in optimizing these sequences.

T. M. Link and B. J. Schwaiger were partially supported by National Institutes of Health grants R01AR064771 and P5AR060752.

References

1. Kumar D, Wyatt CR, Lee S, et al. Association of cartilage defects, and other MRI findings with pain and function in individuals with mild-moderate radiographic hip osteoarthritis and controls. Osteoarthritis Cartilage 2013; 21:1685–1692 [PubMed: 23948977]
2. Gold SL, Burge AJ, Potter HG. MRI of hip cartilage: joint morphology, structure, and composition. Clin Orthop Relat Res 2012; 470:3321–3331 [PubMed: 22723242]
3. Millis MB, Kim YJ. Rationale of osteotomy and related procedures for hip preservation: a review. Clin Orthop Relat Res 2002; 108–121
4. Ganz R, Parvizi J, Beck M, Leunig M, Notzli H, Siebenrock KA. Femoroacetabular impingement: a cause for osteoarthritis of the hip. Clin Orthop RelatRes 2003; 112–120
5. Rubin DA. Femoroacetabular impingement: fact, fiction, or fantasy? AJR 2013; 201:526–534 [PubMed: 23971444]
6. Philippon MJ, Stubbs AJ, Schenker ML, Maxwell RB, Ganz R, Leunig M. Arthroscopic management of femoroacetabular impingement: osteoplasty technique and literature review. Am J Sports Med 2007; 35:1571–1580 [PubMed: 17420508]
7. Mamisch TC, Zilkens C, Siebenrock KA, Bittersohl B, Kim YJ, Werlen S. MRI of hip osteoarthritis and implications for surgery. Radiol Clin North Am 2009; 47:713–722 [PubMed: 19631078]
8. El Bitar YF, Lindner D, Jackson TJ, Domb BG. Joint-preserving surgical options for management of chondral injuries of the hip. J Am Acad Orthop Surg 2014; 22:46–56 [PubMed: 24382879]
9. Hackney LA, Lee MH, Joseph G, Link TM. Subchondral insufficiency fractures of the femoral head: associated morphological findings, longitudinal evolution, and management strategies, (abstr) In: Proceedings of the European Congress of Radiology! annual meeting Vienna, Austria: Springer, 2015
10. Bucknor MD, Nardo L, Joseph GB, et al. Association of cartilage degeneration with four year weight gain: 3T MRI data from the Osteoarthritis Initiative. Osteoarthritis Cartilage 2015; 23:525–531 [PubMed: 25591445]
11. Teichtahl AJ, Smith S, Wang Y, et al. Occupational risk factors for hip osteoarthritis are associated with early hip structural abnormalities: a 3.0T magnetic resonance imaging study of community-based adults. Arthritis Res Ther 2015; 17:19 [PubMed: 25627648]
12. Serebrakian AT, Poulos T, Liebl H, et al. Weight loss over 48 months is associated with reduced progression of cartilage T2. relaxation time values: data from the Osteoarthritis Initiative. J Magn Reson Imaging 2015; 41:1272–1280 [PubMed: 24700497]
13. Wyler A, Bousson V, Bergot C, et al. Hyaline cartilage thickness in radiographically normal cadaveric hips: comparison of spiral CT arthrographic and macroscopic measurements. Radiology 2007; 242:441–449 [PubMed: 17255415]
14. Link TM. MR imaging in osteoarthritis: hardware, coils, and sequences. Magn Reson Imaging Clin N Am 2010; 18:95–110 [PubMed: 19962095]
15. Mamisch TC, Bittersohl B, Hughes T, et al. Magnetic resonance imaging of the hip at 3 Tesla: clinical value in femoroacetabular impingement of the hip and current concepts. Semin Musculoskelet Radiol 2008; 12:212–222 [PubMed: 18850503]
16. Peterfy CG, Gold G, Eckstein F, Cicuttini F, Dardzinski B, Stevens R. MRI protocols for whole-organ assessment of the knee in osteoarthritis. Osteoarthritis Cartilage 2006; 14(suppl A):A95–A111 [PubMed: 16750915]
17. Hayashi D, Roemer FW, Guermazi A. Choice of pulse sequences for magnetic resonance imaging-based semiquantitative assessment of cartilage defects in osteoarthritis research: comment on the article by Dore et al. Arthritis Rheum 2010; 62:3830–3831, author reply 3831–3832 [PubMed: 20812337]
18. Link TM, Stahl R, Woertler K. Cartilage imaging: motivation, techniques, current and future significance. Eur Radiol 2007; 17:1135–1146 [PubMed: 17093967]
19. Link T MRI of cartilage: standard techniques In: Link TM, ed. Cartilage imaging. New York, NY: Springer, 2011:49–66

20. Riley GM, McWalter EJ, Stevens KJ, Safran MR, Lattanzi R, Gold GE. MRI of the hip for the evaluation of femoroacetabular impingement; past, present, and future. J Magn Reson Imaging 2015; 41:558–572 [PubMed: 25155435]
21. Lee S, Nardo L, Kumar D, et al. Scoring hip osteoarthritis with MRI (SHOMRI): a whole joint osteoarthritis evaluation system. J Magn Reson Imaging 2015; 41:1549–1557 [PubMed: 25139720]
22. Roemer FW, Kwoh CK, Hannon MJ, et al. Semiquantitative assessment of focal cartilage damage at 3T MRI: a comparative study of dual echo at steady state (DESS) and intermediate-weighted (IW) fat suppressed fast spin echo sequences. Eur J Radiol 2011; 80:e126–e131 [PubMed: 20833493]
23. Peterfy CG, Schneider E, Nevitt M. The osteoarthritis initiative: report on the design rationale for the magnetic resonance imaging protocol for the knee. Osteoarthritis Cartilage 2008; 16:1433–1441 [PubMed: 18786841]
24. Potter HG, Schachar J. High resolution noncontrast MRI of the hip. J Magn Reson Imaging 2010; 31:268–278 [PubMed: 20099338]
25. Sonin AH, Pensy RA, Mulligan ME, Hatem S. Grading articular cartilage of the knee using fast spin-echo proton density-weighted MR imaging without fat suppression. AJR 2002; 179: 1159–1166 [PubMed: 12388492]
26. Shapiro L, Harish M, Hargreaves B, Staroswiecki E, Gold G. Advances in musculoskeletal MRI: technical considerations. J Magn Reson Imaging 2012; 36:775–787 [PubMed: 22987756]
27. Lazik A, Korsmeier K, Classen T, et al. 3 Tesla high-resolution and delayed gadolinium enhanced MR imaging of cartilage (dGEMRIC) after autologous chondrocyte transplantation in the hip. J Magn Reson Imaging 2014 12 9 [Epub ahead of print]
28. Kijowski R, Davis KW, Woods MA, et al. Knee joint: comprehensive assessment with 3D isotropic resolution fast spin-echo MR imaging: diagnostic performance compared with that of conventional MR imaging at 3.0 T. Radiology 2009; 252:486–495 [PubMed: 19703886]
29. Li CQ, Chen W, Rosenberg JK, et al. Optimizing isotropic three-dimensional fast spin-echo methods for imaging the knee. J Magn Reson Imaging 2014; 39:1417–1425 [PubMed: 24987753]
30. Glaser C, Burgkart R, Kutschera A, Englmeier KH, Reiser M, Eckstein F. Femoro-tibial cartilage metrics from coronal MR image data: technique, test-retest reproducibility, and findings in osteoarthritis. Magn Reson Med 2003; 50:1229–1236 [PubMed: 14648571]
31. Recht MP, Piraino DW, Paletta GA, Schils JP, Belhobek GH. Accuracy of fat-suppressed three-dimensional spoiled gradient-echo FLASH MR imaging in the detection of patellofemoral articular cartilage abnormalities. Radiology 1996; 198:209–212 [PubMed: 8539380]
32. Hardy PA, Recht MP, Piraino D, Thomasson D. Optimization of a dual echo in the steady state (DESS) free-precession sequence for imaging cartilage. J Magn Reson Imaging 1996; 6:329–335 [PubMed: 9132098]
33. Fujinaga Y, Yoshioka H, Sakai T, Sakai Y, Souza F, Lang P. Quantitative measurement of femoral condyle cartilage in the knee by MRI: validation study by multireaders. J Magn Reson Imaging 2014; 39:972–977 [PubMed: 24123712]
34. Bittersohl B, Miese FR, Hosalkar HS, et al. T2* mapping of hip joint cartilage in various histological grades of degeneration. Osteoarthritis Cartilage 2012; 20:653–660 [PubMed: 22469845]
35. Kijowski R, Gold GE. Routine 3D magnetic resonance imaging of joints. J Magn Reson Imaging 2011; 33:758–771 [PubMed: 21448939]
36. Yoshioka H, Stevens K, Genovese M, Dillingham MF, Lang P. Articular cartilage of knee: normal patterns at MR imaging that mimic disease in healthy subjects and patients with osteoarthritis. Radiology 2004; 231:31–38 [PubMed: 15068938]
37. Hong RJ, Hughes TH, Gentili A, Chung CB. Magnetic resonance imaging of the hip. J Magn Reson Imaging 2008; 27:435–445 [PubMed: 18183574]
38. Zalavras CG, Lieberman JR. Osteonecrosis of the femoral head: evaluation and treatment. J Am Acad Orthop Surg 2014; 22:455–464 [PubMed: 24966252]

39. Byrd JW, Jones KS. Diagnostic accuracy of clinical assessment, magnetic resonance imaging, magnetic resonance arthrography, and intra-articular injection in hip arthroscopy patients. Am J Sports Med 2004; 32:1668–1674 [PubMed: 15494331]
40. Sutter R, Zubler V, Hoffmann A, et al. Hip MRI: how useful is intraarticular contrast material for evaluating surgically proven lesions of the labrum and articular cartilage? AJR 2014; 202:160–169 [PubMed: 24370140]
41. McCarthy JC, Glassner PJ. Correlation of magnetic resonance arthrography with revision hip arthroscopy. Clin Orthop Relat Res 2013; 471:4006–4011 [PubMed: 23904247]
42. Smith TO, Simpson M, Ejindu V, Hing CB. The diagnostic test accuracy of magnetic resonance imaging, magnetic resonance arthrography and computer tomography in the detection of chondral lesions of the hip. Eur J Orthop Surg Traumatol 2013; 23:335–344 [PubMed: 23412284]
43. Schmaranzer F, Klauser A, Kogler M, et al. Diagnostic performance of direct traction MR arthrography of the hip: detection of chondral and labral lesions with arthroscopic comparison. Eur Radiol 2015; 25:1721–1730 [PubMed: 25465714]
44. Zhang M, Min Z, Rana N, Liu H. Accuracy of magnetic resonance imaging in grading knee chondral defects. Arthroscopy 2013; 29:349–356 [PubMed: 22906758]
45. Buckwalter JA, Mankin HJ, Grodzinsky AJ. Articular cartilage and osteoarthritis. Instr Course Lect 2005; 54:465–480 [PubMed: 15952258]
46. Siebelt M, Agricola R, Weinans H, Kim YJ. The role of imaging in early hip OA. Osteoarthritis Cartilage 2014; 22:1470–1480 [PubMed: 25278058]
47. Palmer AJ, Brown CP, McNally EG, et al. Noninvasive imaging of cartilage in early osteoarthritis. Bone Joint J 2013; 95B:738–746
48. Bashir A, Gray ML, Hartke J, Burstein D. Nondestructive imaging of human cartilage glycosaminoglycan concentration by MRI. Magn Reson Med 1999; 41:857–865 [PubMed: 10332865]
49. Watanabe A, Wada Y, Obata T, et al. Delayed gadolinium-enhanced MR to determine glycosaminoglycan concentration in reparative cartilage after autologous chondrocyte implantation: preliminary results. Radiology 2006; 239:201–208 [PubMed: 16484349]
50. Jungmann PM, Baum T, Bauer JS, et al. Cartilage repair surgery: outcome evaluation by using noninvasive cartilage biomarkers based on quantitative MRI techniques? Biomed Res Int 2014; 2014:840170 [PubMed: 24877139]
51. Crema MD, Roemer FW, Marra MD, et al. Articular cartilage in the knee: current MR imaging techniques and applications in clinical practice and research. RadioGraphics 2011; 31:37–61 [PubMed: 21257932]
52. Bittersohl B, Hosalkar HS, Haamberg T, et al. Reproducibility of dGEMRIC in assessment of hip joint cartilage: a prospective study. J Magn Reson Imaging 2009; 30:224–228 [PubMed: 19557744]
53. Akella SV, Regatte RR, Gougoutas AJ, et al. Proteoglycan-induced changes in T1rho-relaxation of articular cartilage at 4T. Magn Reson Med 2001; 46:419–423 [PubMed: 11550230]
54. Wang L, Regatte RR. T1rho MRI of human musculoskeletal system. J Magn Reson Imaging 2015; 41:586–600 [PubMed: 24935818]
55. Kim YJ. Novel cartilage imaging techniques for hip disorders. Magn Reson Imaging Clin N Am 2013; 21:35–44 [PubMed: 23168181]
56. Rakhra KS, Cardenas-Blanco A, Melkus G, Schweitzer ME, Cameron IG, Beaule PE. Is the T1rho MRI profile of hyaline cartilage in the normal hip uniform? Clin Orthop Relat Res 2015; 473:1325–1332 [PubMed: 25082625]
57. Subburaj K, Valentinitsch A, Dillon AB, et al. Regional variations in MR relaxation of hip joint cartilage in subjects with and without femoroace tabular impingement. Magn Reson Imaging 2013; 31:1129–1136 [PubMed: 23684960]
58. Levitt M Spin dynamics: basics of nuclear magnetic resonance. New York, NY: Wiley, 2008
59. Nishii T, Tanaka H, Sugano N, Sakai T, Hananouchi T, Yoshikawa H. Evaluation of cartilage matrix disorders by T2 relaxation time in patients with hip dysplasia. Osteoarthritis Cartilage 2008; 16:227–233 [PubMed: 17644363]

60. Wei B, Gu Q, Li D, et al. Mild degenerative changes of hip cartilage in elderly patients: an available sample representative of early osteoarthritis. Int J Clin Exp Pathol 2014; 7:6493–6503 [PubMed: 25400727]
61. Bittersohl B, Hosalkar HS, Hughes T, et al. Feasibility of T2* mapping for the evaluation of hip joint cartilage at 1.5T using a three-dimensional (3D), gradient-echo (GRE) sequence: a prospective study. Magn Reson Med 2009; 62:896–901 [PubMed: 19645008]
62. Bittersohl B, Miese FR, Hosalkar HS, et al. T2* mapping of acetabular and femoral hip joint cartilage at 3 T: a prospective controlled study. Invest Radiol 2012; 47:392–397 [PubMed: 22627944]
63. Apprich S, Mamisch TC, Welsch GH, et al. Evaluation of articular cartilage in patients with femoroacetabular impingement (FAI) using T2* mapping at different time points at 3.0 Tesla MRI: a feasibility study. Skeletal Radiol 2012; 41:987–995 [PubMed: 22057581]
64. Noyes FR, Stabler CL. A system for grading articular cartilage lesions at arthroscopy. Am J Sports Med 1989; 17:505–513 [PubMed: 2675649]
65. Outerbridge RE. The etiology of chondromalacia patellae. J Bone Joint Surg Br 1961; 43:752–757 [PubMed: 14038135]
66. Kumar D, Dillon A, Nardo L, Link TM, Majumdar S, Souza RB. Differences in the association of hip cartilage lesions and cam-type femoroacetabular impingement with movement patterns: a preliminary study. PM R 2014; 6:681–689 [PubMed: 24534097]
67. Duc SR, Koch P, Schmid MR, Horger W, Hodler J, Pfirrmann CW. Diagnosis of articular cartilage abnormalities of the knee: prospective clinical evaluation of a 3D water-excitation true FISP sequence. Radiology 2007; 243:475–482 [PubMed: 17400759]
68. Guermazi A, Roemer FW, Haugen IK, Crema MD, Hayashi D. MRI-based semiquantitative scoring of joint pathology in osteoarthritis. Nat Rev Rheumatol 2013; 9:236–251 [PubMed: 23321609]
69. Neumann G, Mendicuti AD, Zou KH, et al. Prevalence of labral tears and cartilage loss in patients with mechanical symptoms of the hip: evaluation using MR arthrography. Osteoarthritis Cartilage 2007; 15:909–917 [PubMed: 17383908]
70. Roemer FW, Hunter DJ, Winterstein A, et al. Hip Osteoarthritis MRI Scoring System (HOAMS): reliability and associations with radiographic and clinical findings. Osteoarthritis Cartilage 2011; 19:946–962 [PubMed: 21550411]
71. Ilizaliturri VM Jr, Byrd JW, Sampson TG, et al. A geographic zone method to describe intra-articular pathology in hip arthroscopy: cadaveric study and preliminary report. Arthroscopy 2008; 24:534–539 [PubMed: 18442685]
72. Ito K, Minka MA 2nd, Leunig M, Werlen S, Ganz R. Femoroacetabular impingement and the cam-effect: a MRI-based quantitative anatomical study of the femoral head-neck offset. J Bone Joint Surg Br 2001; 83:171–176 [PubMed: 11284559]
73. Yoon LS A, Belzile E, Connolly SA, Millis MB, Palmer WE. Triad of MR arthrographic findings in patients with cam-type femoroacetabular impingement. Radiology 2005; 236:588–592 [PubMed: 15972331]
74. Sutter R, Dietrich TJ, Zingg PO, Pfirrmann CW. How useful is the alpha angle for discriminating between symptomatic patients with cam-type femoroacetabular impingement and asymptomatic volunteers? Radiology 2012; 264:514–521 [PubMed: 22653190]
75. Sutter R, Zanetti M, Pfirrmann CW. New developments in hip imaging. Radiology 2012; 264:651–667 [PubMed: 22919039]
76. Pfirrmann CW, Duc SR, Zanetti M, Dora C, Hodler J. MR arthrography of acetabular cartilage delamination in femoroacetabular cam impingement. Radiology 2008; 249:236–241 [PubMed: 18682585]
77. Konan S, Rayan F, Meermans G, Witt J, Haddad FS. Validation of the classification system for acetabular chondral lesions identified at arthroscopy in patients with femoroacetabular impingement. J Bone Joint Surg Br 2011; 93:332–336 [PubMed: 21357954]
78. Anderson LA, Peters CL, Park BB, Stoddard GJ, Erickson JA, Crim JR. Acetabular cartilage delamination in femoroacetabular impingement: risk factors and magnetic resonance imaging diagnosis. J Bone Joint Surg Am 2009; 91:305–313 [PubMed: 19181974]

79. Lequesne M, Bellaiche L. Anterior femoroacetabular impingement: an update. Joint Bone Spine 2012; 79:249–255 [PubMed: 22281229]

80. Pfirrmann CW, Mengiardi B, Dora C, Kalberer F, Zanetti M, Hodler J. Cam and pincer femoroacetabular impingement: characteristic MR arthrographic findings in 50 patients. Radiology 2006; 240:778–785 [PubMed: 16857978]

81. Domb BG, Jackson TJ, Carter CC, Jester JR, Finch NA, Stake CE. Magnetic resonance imaging findings in the symptomatic hips of younger retired National Football League players. Am J Sports Med 2014; 42:1704–1709 [PubMed: 24780892]

82. Khanna V, Harris A, Farrokhyar F, Choudur HN, Wong IH. Hip arthroscopy: prevalence of intraarticular pathologic findings after traumatic injury of the hip. Arthroscopy 2014; 30:299–304 [PubMed: 24581254]

83. Tehranzadeh J, Vanarthos W, Pais MJ. Osteochondral impaction of the femoral head associated with hip dislocation: CT study in 35 patients. AJR 1990; 155:1049–1052 [PubMed: 2120934]

84. Bohndorf K Imaging of acute injuries of the articular surfaces (chondral, osteochondral and subchondral fractures). Skeletal Radiol 1999; 28:545–560 [PubMed: 10550531]

85. Nevitt MC. Definition of hip osteoarthritis for epidemiological studies. Ann Rheum Dis 1996; 55:652–655 [PubMed: 8882141]

86. Teichtahl AJ, Wang Y, Smith S, et al. Structural changes of hip osteoarthritis using magnetic resonance imaging. Arthritis Res Ther 2014; 16:466 [PubMed: 25304036]

87. Gossec L, Tubach F, Baron G, Ravaud P, Logeart I, Dougados M. Predictive factors of total hip replacement due to primary osteoarthritis: a prospective 2 year study of 505 patients. Ann Rheum Dis 2005; 64:1028–1032 [PubMed: 15640268]

88. Yamamoto T, Bullough PG. The role of subchondral insufficiency fracture in rapid destruction of the hip joint: a preliminary report. Arthritis Rheum 2000; 43:2423–2427 [PubMed: 11083264]

89. Davies M, Cassar-Pullicino VN, Darby AJ. Subchondral insufficiency fractures of the femoral head. Eur Radiol 2004; 14:201–207 [PubMed: 12851782]

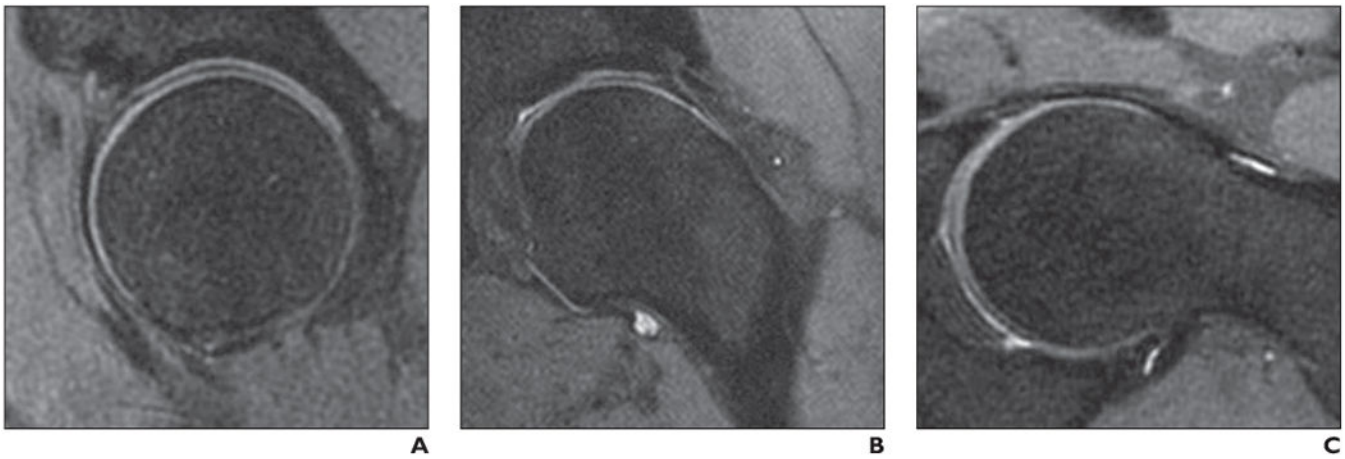

Fig. 1—.

Left hip of healthy volunteer. (Courtesy of Han M and Krug R, University of California at San Francisco, San Francisco, CA)

A–C, Sagittal (**A**), coronal (**B**), and obligue axial (**C**) reformation images (slice thickness, 2 mm) of 3D intermediate-weighted fast spin-echo seguence (Cube, GE Healthcare) originally obtained with 0.8 × 0.8 × 0.8 mm^3 isotropic spatial resolution and 7-minute acguisition time. In this study, both acetabular cartilage and femoral cartilage are well delineated.

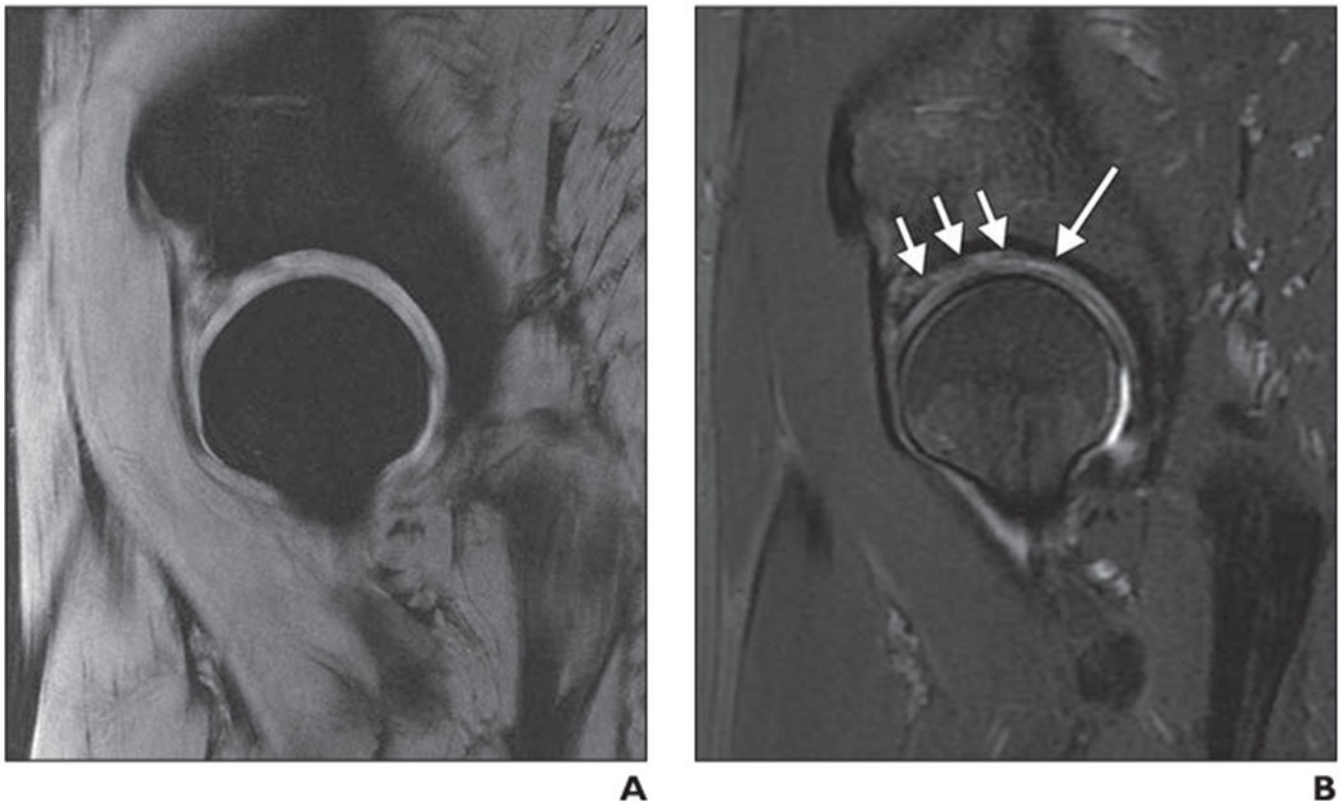

Fig. 2—.

Right hip of 50-year-old woman with osteoarthritis.

A and **B**, Spoiled T2*-weighted MERGE (Multiple Echo Recombined Gradient Echo, GE Healthcare) image (**A**) and 2D intermediate-weighted fast spin-echo (FSE) image (**B**). MERGE image provides good separation of acetabular cartilage and femoral cartilage; however, both partial-thickness focal acetabular cartilage lesion (*long arrow*, **B**) and cartilage signal inhomogeneity (*short arrows*, **B**), which are clearly shown on 2D FSE image, are insufficiently depicted on MERGE image.

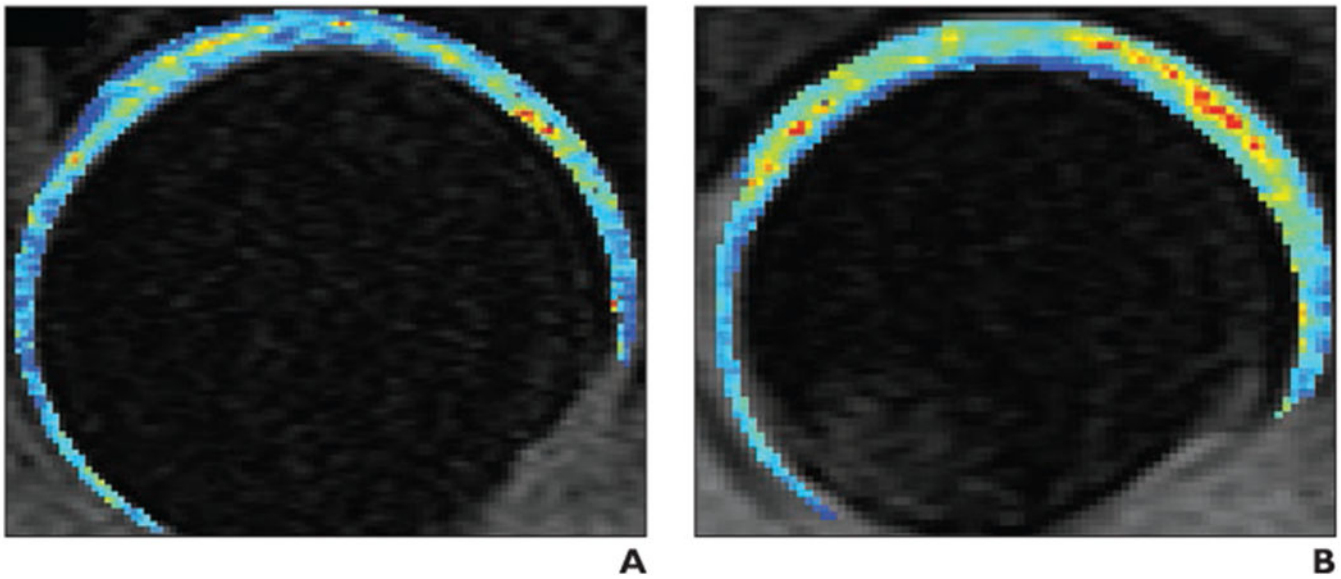

Fig. 3—.

T1rho color maps of acetabular cartilage and femoral cartilage. (Courtesy of Samaan M and Souza RB, University of California at San Francisco, San Francisco, CA)

A and **B**, Composite T1rho color maps of both acetabular cartilage and femoral cartilage of left hip obtained in sagittal plane in healthy 35-year-old control subject (**A**) and 30-year-old woman with early hip osteoarthritis (**B**). T1rho values are elevated (yellow, orange, and red) in weight-bearing regions of osteoarthritis patient (in particular, in superolateral and superomedial acetabular and femoral cartilage), indicating changes in regional proteoglycan composition. Also note that patient (**B**) does not have joint space narrowing and that joint space appears mildly widened compared with control subject (**A**); joint space widening in patient potentially reflects cartilage swelling. Blue and green = normal T1rho values.

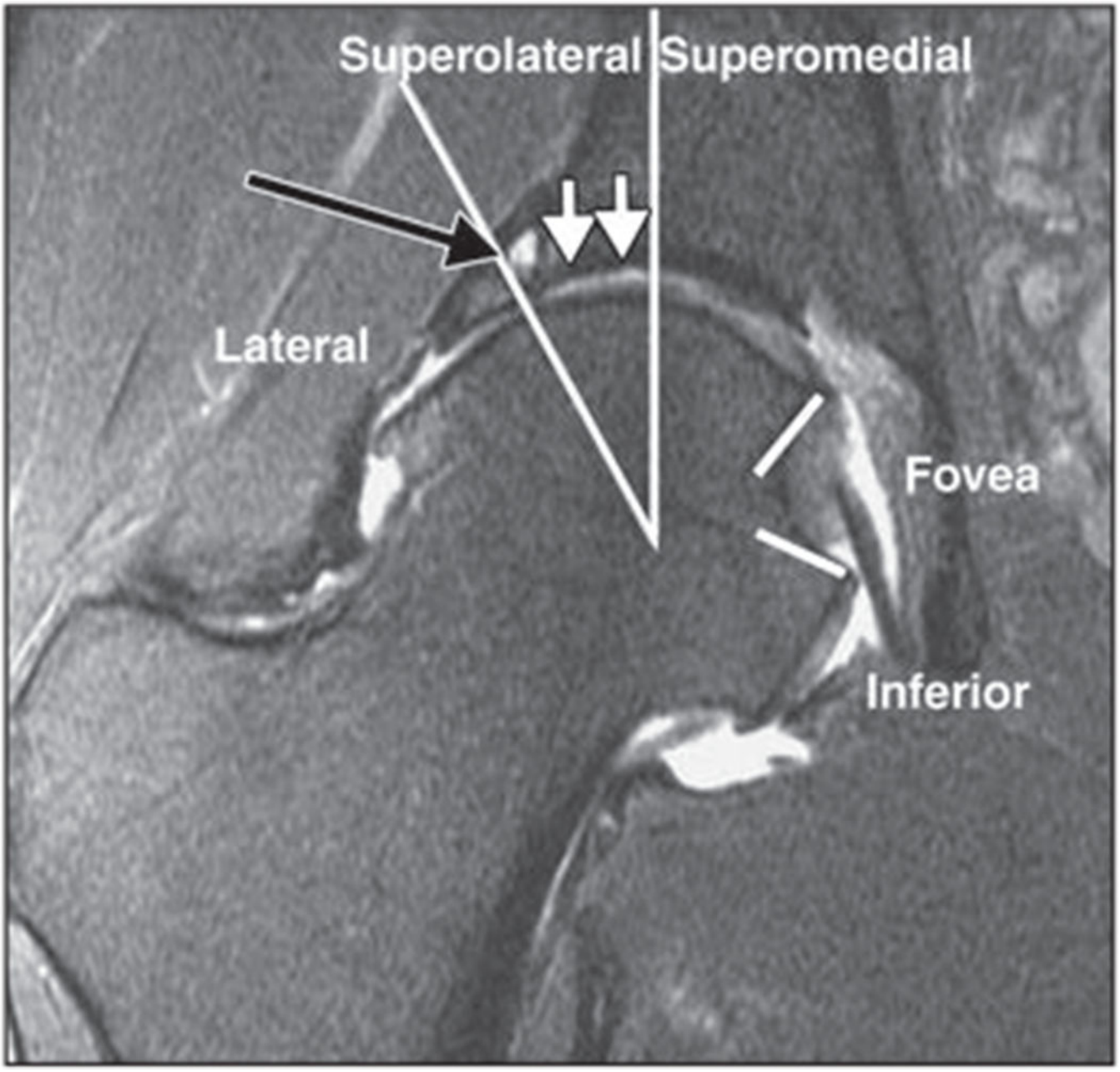

Fig. 4—.

Coronal 2D fat-suppressed intermediate-weighted fast spin-echo image of right hip of 42-year-old woman with degenerative disease of hip and femoroacetabular impingement. According to score obtained using SHOMRI (scoring hip osteoarthritis with MRI) scoring system [21], femoral cartilage is separated into four subregions and acetabular cartilage into three subregions in coronal image. There is full-thickness acetabular cartilage loss with diameter of 10 mm (*white arrows*) in superolateral subregion, which would be scored as grade 2 lesion according to SHOMRI. There is also subchondral cyst (*black arrow*) in superolateral region. Findings were arthroscopically confirmed. Long lines show separate lateral, superolateral, and superomedial regions, and short lines = indicate foveal regions.

Fig. 5—.

MR arthrography of right hip of 40-year-old man with clinical diagnosis of femoroacetabular impingement (FAI).

A, Coronal T1-weighted fat-suppressed (FS) fast spin-echo (FSE) image shows focal cartilage defect (*long arrow*) at acetabular cartilage in direct proximity to labral insertion and osteophyte (*short arrow*) at margin of femoral head.

B, Coronal T1-weighted FS FSE image shows additional cartilage delamination at acetabulum (*long arrow*) and marginal osteophytes (*short arrows*).

C, Oblique axial intermediate-weighted FS FSE image shows typical deformity (asphericity) of femoral head with prominence at head-neck junction (*long arrow*) along with diffuse cartilage loss (*short arrows*). Patient underwent arthroscopic FAI surgery, which verified cartilage delamination.

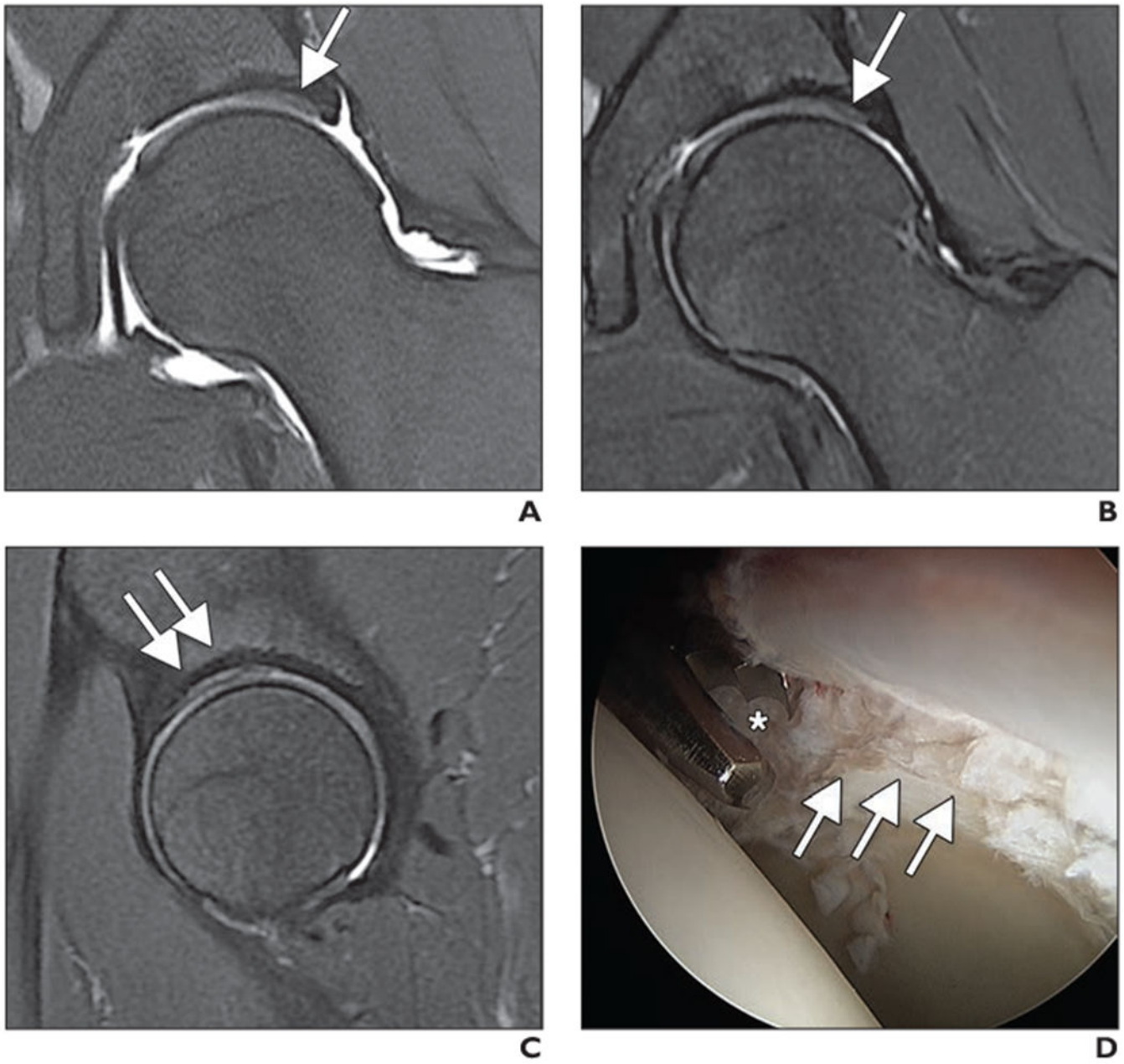

Fig. 6—.

MR arthrography of left hip of 26-year-old man with clinical diagnosis of femoroacetabular impingement.

A and **B**, Unenhanced coronal intermediate-weighted fat-saturated fast spin-echo (FSE) MR arthrograms obtained at 1.5 T (**A**) and at 1.5 T, unehanced 3-T MRI, and arthroscopy at 3T (**B**) show area of bright signal intensity along superior acetabulum with adjacent darker hypointense cartilage (*arrow*) consistent with delamination.

C, Sagittal intermediate-weighted fat-saturated FSE image obtained at 3 T shows findings (*arrows*) similar to coronal images (**A** and **B**).

D, Arthroscopic image shows acetabular cartilage delamination (*arrows*) with injured cartilage layer being débrided by arthroscopic biter (*asterisk*).

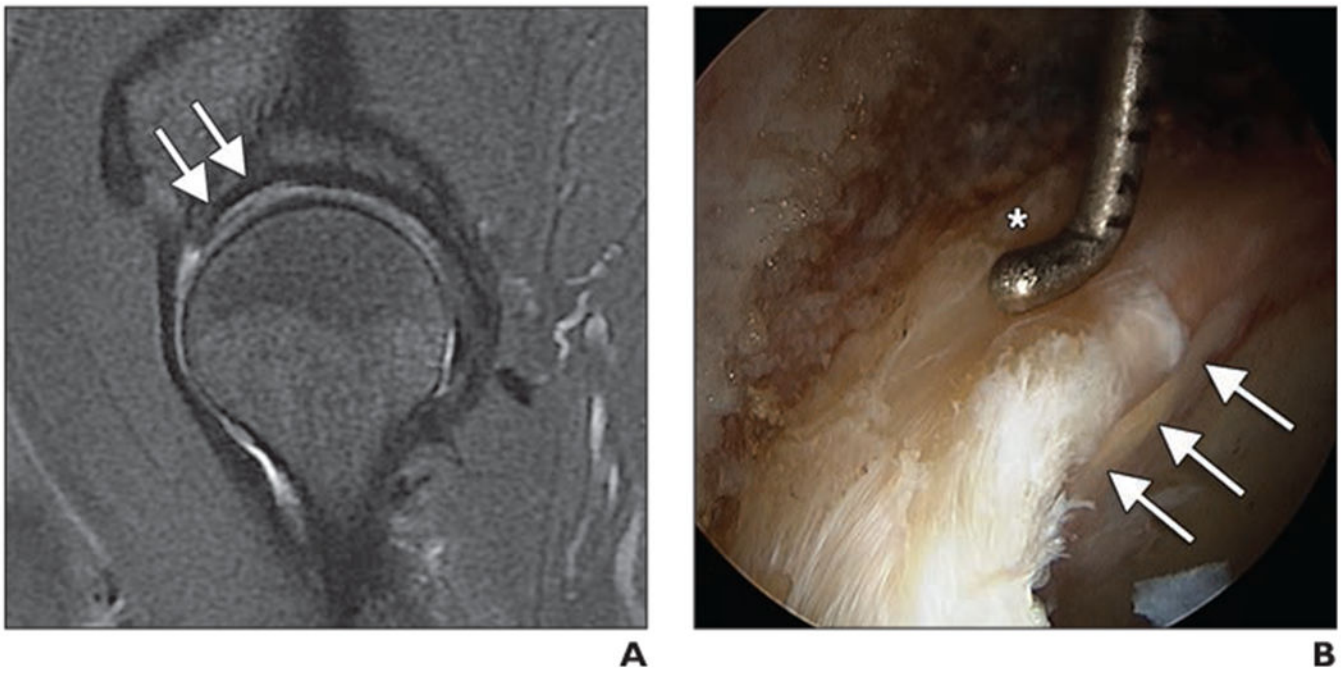

Fig. 7—.

Cartilage delamination in 55-year-old man with clinical signs of femoroacetabular impingement.

A, Sagittal intermediate-weighted fat-saturated fast spin-echo (FSE) image obtained at 3 T shows abnormal cartilage at acetabulum with bright signal intensity along subchondral bone and layer of darker hypointense cartilage covering this area (*arrows*).

B, Arthroscopic image shows acetabular cartilage delamination at chondrolabral junction as pressure applied to labrum by arthroscopic probe (*asterisk*) causes positive wave sign to underlying delaminated cartilage (*arrows*).

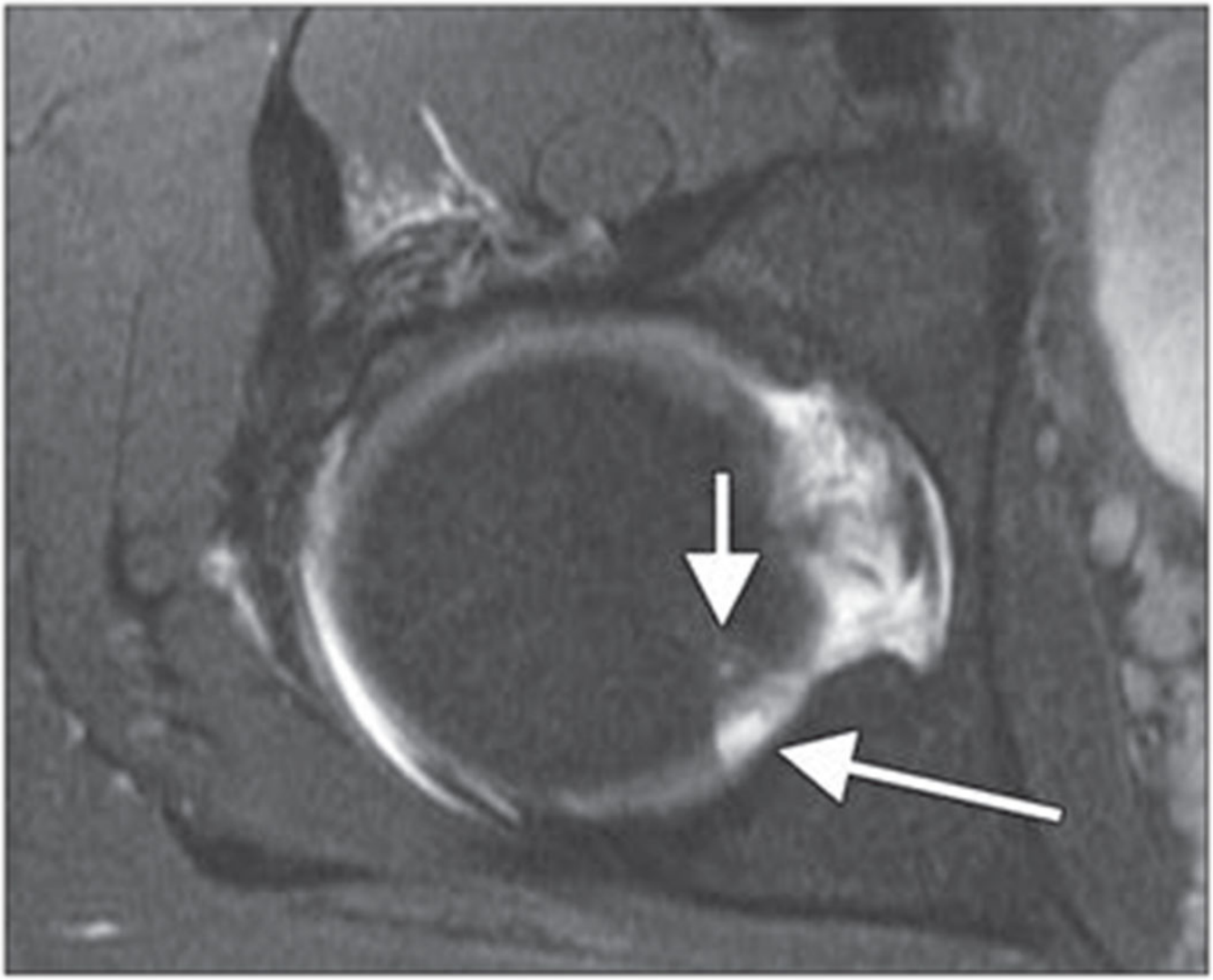

Fig. 8—.

Axial intermediate-weighted fat-suppressed fast spin-echo image of right femoral head shows posttraumatic focal cartilage defect (*long arrow*) at posterior aspect of femoral head with some adjacent mild bone marrow signal abnormalities (*short arrow*).

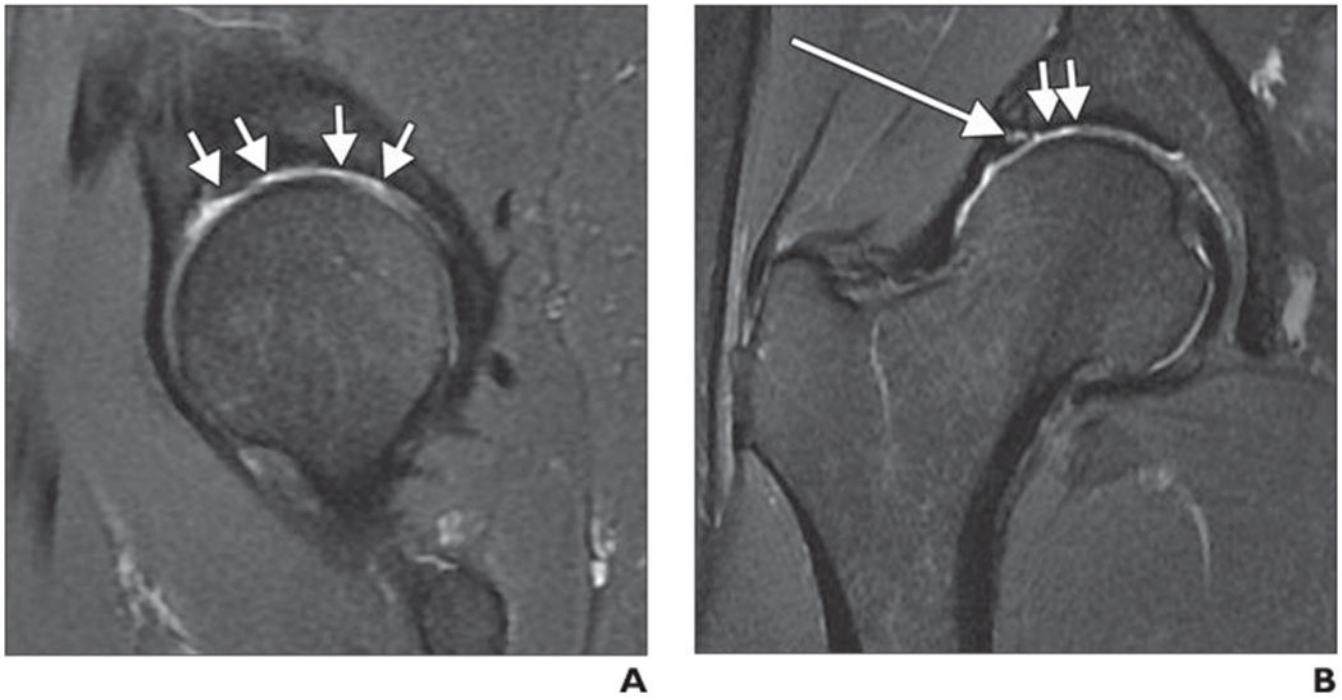

Fig. 9—.

42-year-old man with moderate hip osteoarthritis characterized by joint space narrowing. **A** and **B**, Sagittal (**A**) and coronal (**B**) intermediate-weighted fat-suppressed fast spin-echo images show diffuse cartilage loss in weight-bearing central and anterior regions of acetabulum (*arrows*, **A**) and in superolateral region (*short arrows*, **B**). Also, note labral tear (*long arrow*, **B**).

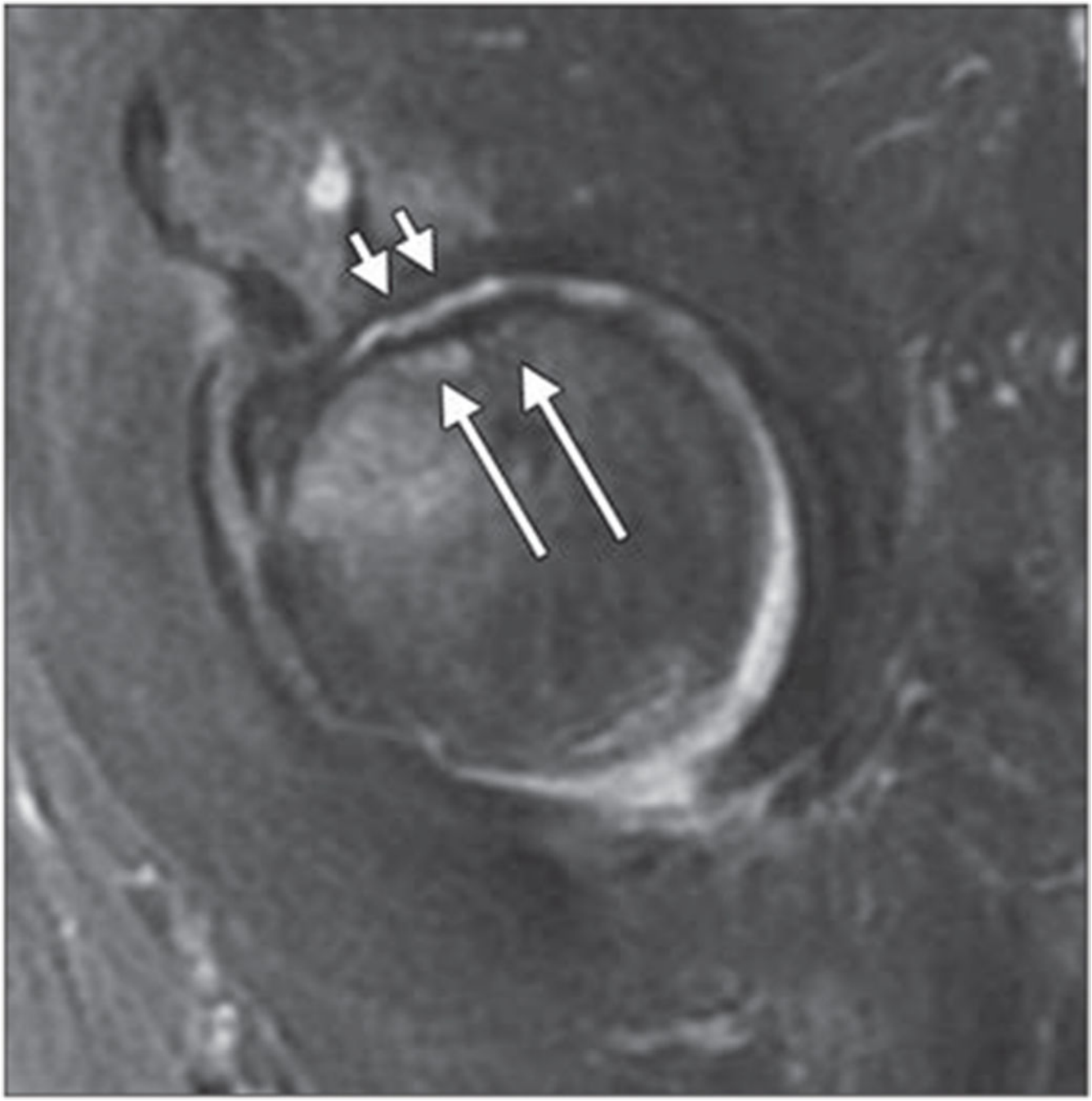

Fig. 10—.

Sagittal intermediate-weighted fat-suppressed fast spin-echo image of 65-year-old woman shows femoral head subchondral insufficiency fracture (*long arrows*) and joint space narrowing. Diffuse cartilage lossisseen in weight-bearing central and anterior regions of acetabulum and femoral head (*short arrows*). There is also mild bone marrow edema pattern in femoral head adjacent to fracture.

TABLE 1:

Recommended Sequence Parameters for MRI of the Cartilage of the Hip Joint and for MR Arthrography of the Hip Joint

Parameter	3-T MRI (1.5-T MRI)		
	Intermediate-Weighted and T2-Weighted Fat Suppressed	T1-Weighted Fat Suppressed FSE[a]	T1-Weighted FSE
Orientation	Coronal, oblique axial, sagittal	Coronal	Coronal
TR range (ms)	4000–5000 (4000–5000)	650–950 (650–950)	600–800 (600–800)
TE (ms)	~ 55 (~ 45)	10–20 (10–20)	10–20 (10–20)
Fat suppression	Yes (yes)	Yes (yes)	No (no)
Receiver bandwidth (Hz/pixel)	31 (16)	31 (16)	31 (21)
ETL	14(14)	4–6 (4–6)	3–4 (3–4)
No. of signals acquired	4 (4)	4 (4)	4 (4)
FOV (cm)	16(18)	16(18)	16(18)
Matrix	320 × 224 (320 × 224)	288 × 192 (288 × 192)	352 × 224 (352 × 224)
Slice (mm)	3–4 (4)	3–4 (4)	3–4 (4)
Gap (mm)	0 (0)	0 (0)	0 (0)
Acquisition time (min:s)	~4:30 (~ 4:30)	~5:00 (~ 5:00)	~5:30 (~ 5:30)

Note—For all examinations, an 8-channel cardiac coil was used, the patient was imaged feet first in the supine position, and 20 slices were obtained. FSE = fast spin-echo, ETL = echo-train length.

[a]For MR arthrography only

TABLE 2:

Cartilage Evaluation by Semiquantitative Whole-Organ Scoring Systems for Hip Osteoarthritis

Characteristics of MRI and Scoring Systems	Neumann et al. [69]	HOAMS [63]	SHOMRI [12]
Sequences	Sagittal, coronal, and axial T1-weighted fat-saturated spin-echo sequence after direct injection of gadopentetate dimeglumine	Sagittal and coronal proton density–weighted FS FSE sequence and sagittal 2D MEDIC sequence	Sagittal, oblique coronal, and oblique axial intermediate-weighted FS FSE sequence
B_0 field strength (T)	1.5	1.5	3
Concept of subregional division	One central subregion and four symmetric radially separated regions	Composite regional scores both for acetabular and femoral cartilage: anterior and posterior regions encompassing 9–10 mm of anterior and posterior femoral head, respectively, as shown in sagittal images; subdivision of central region in subregions follows both anatomic landmarks and geometric measurements	Anterior and posterior regions encompassing 1 cm of anterior and posterior femoral head, respectively, as shown in sagittal images; subdivision of midportion follows anatomic landmarks
Division of acetabular cartilage	5 Subregions: anterior, posterior, central, medial, lateral	9 Subregions, scored together for acetabular and femoral cartilage: anterior-superior, anteroinferior, central-lateral, central-superior, central-central, central-inferior, central-medial, posterior-superior, posterior-inferior	4 Subregions: anterior, superolateral, superomedial, posterior
Division of femoral cartilage	5 Subregions: anterior, posterior, central, medial, lateral	Graded together with acetabular cartilage	6 Subregions: anterior, lateral, superolateral, superomedial, inferior, posterior
Cartilage scoring per subregion	0 = normal, 1 = signal heterogeneity, 2 = fissuring < 1 mm, 3 = thinning < 50%, 4 = thinning > 50%, 5 = full-thickness loss	0 = normal cartilage, 1 = focal partial-thickness defect (< 25% of subregional area), 2 = focal full-thickness defect (≤ 25% of subregional area), 3 = several partial-thickness defects or a single but larger superficial defect (≤ 25% of subregional area), 4 = several large full-thickness defects or single but full-thickness defect (> 25% of subregional area)	0 = no cartilage thickness loss, 1 = partial-thickness loss, 2 = full-thickness loss
Cartilage lesion width scoring	A ≤ 1 cm; B = 1–2 cm; C = 2–3 cm; D = 3–4 cm; E ≥ 4 cm	As part of the subregional score (see above)	Lesions > 1 cm diameter spanning two regions are scored in both regions; smaller lesions are scored in only one region

Note—HOAMS = Hip Osteoarthritis MRI Scoring System, SHOMRI = scoring hip osteoarthritis with MRI, FS = fat-suppressed, FSE = fast spin-echo, MEDIC = Multi-Echo Data Image Combination (Siemens Healthcare).